

Supporting Information

Influence of the backbone of N₅-pentadentate ligands on the catalytic performance of Ni(II) complexes for electrochemical water oxidation in neutral aqueous solutions

Junyu Shen, Mei Wang,* Tianhao He, Jian Jiang and Maowei Hu

State Key Laboratory of Fine Chemicals, Faculty of Chemical, Environmental and Biological Science and Technology, Dalian University of Technology (DUT), Dalian 116024, China.

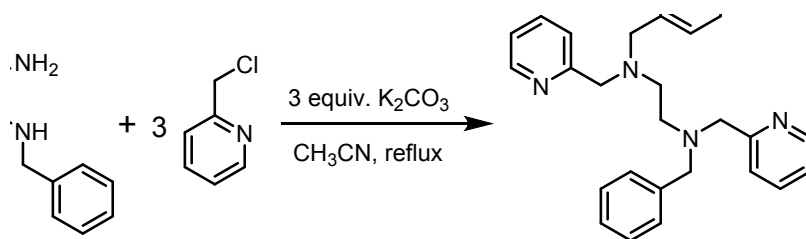
Materials and instruments

Materials. Manipulations for preparation of the nickel complexes were carried out under pure N₂ by using standard Schlenk techniques. Commercially available chemicals, Ni(BF₄)₂·6H₂O, benzaldehyde, 1,2-ethanediamine, 2-(chloromethyl)pyridine hydrochloride, (1*R*,2*R*)-1,2-diaminocyclohexane, and benzyl bromide were purchased from Adamas reagent. Glassy carbon electrodes (GCEs), fluorine-doped tin oxide (FTO) glass plates, and platinum foils were purchased from Tianjin Gauss Union for electrochemical studies. All buffers were prepared with deionized water (18 MΩ-cm resistivity).

Instruments. NMR Spectra were collected with a Varian INOVA 400 NMR spectrometer. Mass spectra were recorded with HP 1100 HPL/ESI-DAD-MS and Waters/Micromass LC/Q-TOF-MS instruments. Elemental analyses were performed with a Thermoquest-Flash EA 1112 elemental analyzer. UV-Vis absorption measurements were carried out on an Agilent 8453 spectrophotometer. SEM images and EDX spectra were obtained with a FEI Nova NanoSEM 450 instrument equipped with an EDX detector. XPS surveys were acquired with a ThermoFisher ESCALAB 250Xi surface analysis system. Dynamic light scattering (DLS) spectra were measured with a Zetasizer Nano ZS90 instrument.

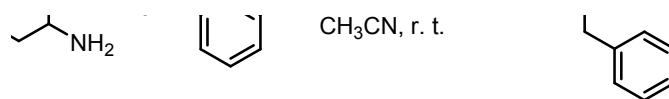
Synthesis

Preparation of L1. *N*-benzyl-*N,N',N'*-tris(pyridin-2-ylmethyl)ethylenediamine (L1) was prepared according to the literature procedure.^{S1} Anal. Calcd for C₂₇H₂₉N₅ (%): C 76.56, H 6.90, N 16.53; found: C 76.65, H 6.83, N 16.60. ¹H NMR (CDCl₃, 400 MHz): δ 8.48 (3H, m), 7.58 (3H, t, *J* = 6.4 Hz), 7.47 (3H, t, *J* = 6.3 Hz), 7.18–7.30 (5H, m), 7.12 (3H, m), 3.77 (4H, s), 3.72 (2H, s), 3.59 (2H, s), and 2.73 (4H, m). ¹³C NMR (CDCl₃, 100 MHz): δ 160.16, 159.73, 148.94, 148.79, 139.18, 136.30, 128.71, 128.17, 126.88, 122.71, 122.65, 121.84, 121.78, 60.78, 60.59, 58.91, 52.20, and 51.89. ESI-MS: Calcd for [M+H]⁺: *m/z* = 424.24; found: *m/z* = 424.21.

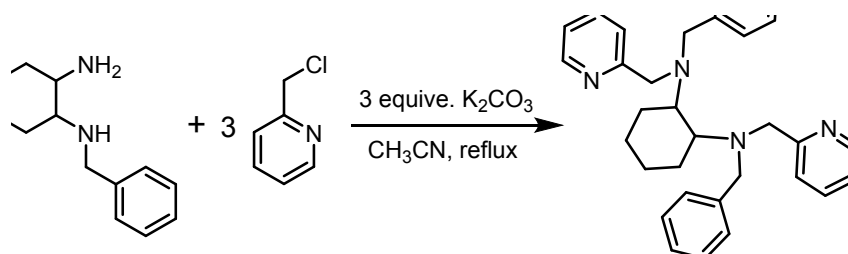


Preparation of (1*R*,2*R*)-*N*-benzyl-1,2-diaminocyclohexane.^{S2} The solution of benzyl bromide (1.46 mL, 10 mmol) in dry acetonitrile (20 mL) was added dropwise into the solution of (1*R*,2*R*)-1,2-diaminocyclohexane (11.41 g, 100 mmol) in CH₃CN (150 mL), and the mixture was stirred at room temperature for 4 h. The solvent was evaporated from the resulting turbid solution, and the residue was extracted with ethyl acetate and saturated NaHCO₃. The combined organic layers were dried over MgSO₄, filtered, and concentrated in vacuo. The crude product was purified by chromatography on a silica gel column with ethyl acetate as eluent. After the solvent was removed by evaporation, the product was obtained as yellow oil in a yield of 90% (1.85 g). ¹H NMR (CDCl₃, 400 MHz): δ 7.22–7.36 (5H, m), 3.94 (1H, d, *J* = 13.0 Hz), 3.69 (1H, d, *J* = 13.1 Hz), 2.38 (1H, m), 2.09 (2H, m), 1.91 (1H, m), 1.73 (2H, m), and 1.09–1.32 (4H, m). ¹³C NMR (CDCl₃, 100 MHz): δ 144.39, 132.11, 130.66, 66.31, 58.21, 54.36, 38.46, 34.37, 28.95, and 28.91. ESI-MS: Calcd for [M+H]⁺: *m/z* = 205.16;

found: $m/z = 205.14$.



Preparation of L2. (1R,2R)-N-benzyl-N,N',N'-tris(pyridin-2-ylmethyl)cyclohexane-1,2-diamine (L2) was prepared with the following method. (1R,2R)-N-benzyl-1,2-diaminocyclohexane (2.04 g, 10 mmol) and 2-(chloromethyl)pyridine (3.81 g, 30 mmol) were dissolved in CH₃CN (100 mL), and K₂CO₃ (4.84 g, 35 mmol) was added to the solution. The mixture was refluxed for 12 h. After the resulting solution was cooled to room temperature, the solid was filtered out, and the solvent was removed by evaporation under vacuum. The crude product was purified by chromatography on a silica gel column with ethyl acetate as eluent. After the solvent was removed by evaporation, the product was obtained as brown oil in a yield of 60% (2.85 g). ¹H NMR (CDCl₃, 400 MHz): δ 8.47 (3H, m), 7.69 (1H, d, $J = 8.0$ Hz), 7.63 (2H, d, $J = 7.6$ Hz), 7.43 (3H, m), 7.32 (2H, d, $J = 7.2$ Hz), 7.07–7.18 (6H, m), 3.73 (3H, m), 3.66 (3H, m), 3.53 (1H, d, $J = 14.5$ Hz), 3.43 (1H, d, $J = 13.7$ Hz), 2.69 (2H, m), 1.72 (2H, m), 1.26 (2H, m), and 1.11 (4H, m). ¹³C NMR (CDCl₃, 100 MHz): δ 160.10, 159.64, 147.77, 147.62, 138.89, 134.90, 127.93, 126.93, 125.73, 122.34, 122.25, 120.70, 120.62, 58.99, 57.90, 54.69, 54.29, 52.77, 24.86, and 23.41. ESI-MS: Calcd for [M+H]⁺: $m/z = 478.29$; found: $m/z = 478.28$.



Preparation of [(L1)Ni(OH₂)](BF₄)₂ (1).^{S3} The salt Ni(BF₄)₂·6H₂O (0.340 g, 1.0 mmol) was added into the aqueous solution (40 mL) of L1 (0.423 g, 1.0 mmol) with magnetic

stirring. The mixture was stirred under nitrogen at room temperature for 8 h. The pink solution was then concentrated to about 10 mL by evaporation under vacuum. After the left solution stood at room temperature for 2 days, pink crystals were obtained in a yield of 83% (0.56 g). Anal. Calcd for $C_{27}H_{31}N_5OB_2F_8Ni \cdot H_2O$ (%): C 46.87, H 4.81, N 10.12; found: C 46.83, H 4.83, N 10.11. TOF-MS: Calcd for $[M - 2BF_4 - H_2O]^{2+}$ ($C_{27}H_{29}N_5Ni$): $m/z = 240.5888$; found: $m/z = 240.5887$.

Preparation of $[(L2)Ni(OH_2)](BF_4)_2$ (2**).** Complex **2** was prepared according to the identical method as that adopted for preparation of **1**, but with ligand L2. Pink crystals were obtained in a yield of 85% (0.62 g). Anal. Calcd for $C_{31}H_{37}N_5B_2F_8NiO$ (%): C 51.15, H 5.12, N 9.62; found: C 51.12, H 5.18, N 9.58. TOF-MS: Calcd for $[M - 2BF_4 - H_2O]^{2+}$ ($C_{31}H_{35}N_5Ni$): $m/z = 267.6123$; found: $m/z = 267.6122$.

Crystallographic structure determinations

The single-crystal X-ray diffraction data were collected on a Bruker Smart Apex II CCD diffractometer with a graphite-monochromated Mo- K_α radiation ($\lambda = 0.071073 \text{ \AA}$) at 296 K using the ω - 2θ scan mode. Data processing was accomplished with the SAINT processing program.^{S4} Intensity data were corrected for absorption by the SADABS program.^{S5} All structures were solved by direct methods and refined on F^2 against full-matrix least-squares methods by using the SHELXTL 97 program package.^{S6} Non-hydrogen atoms were refined anisotropically, and hydrogen atoms were located by geometrical calculation. Crystallographic data and selected bond lengths and angles for **1** and **2** are given in Tables S1 and S2 (CCDC-989007 for **1** and -1839618 for **2**).

Electrochemistry studies

All electrochemical measurements were performed with a model CHI660E electrochemical

workstation (CH instruments).

CV measurements. Cyclic voltammetry experiments were carried out in a three-electrode cell under argon. The working electrode was a glassy carbon electrode disc (0.071 cm²) polished with 3 and 1 μm diamond pastes and sonicated in ion-free water for 15 min prior to use. The reference electrode was an aqueous Ag/AgCl electrode and the counter electrode was a platinum wire. The complex, **1** or **2** (1.0 or 0.5 mM), was completely dissolved in the solution of 0.1 or 0.2 M phosphate buffer at pH 7 as a homogenous electrocatalyst. The solution was degassed by bubbling with argon for 15 min before measurement. Potentials were measured using the Ag/AgCl reference electrode and are reported versus the normal hydrogen electrode (NHE) by addition of 0.197 V to the experimentally measured values.

Controlled potential electrolysis (CPE) experiments. All CPE experiments made in water were carried out in a single cell except for measurements of Faradaic efficiency. A fluorine-doped tin oxide (FTO) with a surface area of 1 cm² was used as the working electrode for electrolysis conducted in aqueous media. The auxiliary electrode was a platinum plate (2 cm²), and the reference electrode was a commercially available aqueous Ag/AgCl electrode. The sample was bubbled with argon for 20 min before measurement.

Determination of Faradaic efficiency. The CPE experiments of the solutions of **1** and **2** (both in 1 mM) were carried out in 0.1 M phosphate buffer (30 mL) at pH 7.0 at an applied potential of 1.62 V vs NHE for 4 h with a FTO (surface area 1 cm²) as the working electrode, a Pt plate (2 cm²) as the auxiliary electrode, and a Ag/AgCl electrode as the reference electrode in a custom built gas-tight one-compartment electrochemical cell. The gas in the headspace of the cell was analyzed during the electrolysis by CEAULIGHT GC-7920 gas chromatograph equipped with a 5 Å molecular sieve column (2 mm × 2 m) and with Ar as carrier gas. For estimation of O₂ leaked into the cell, the sample of air was also analyzed by GC analysis under the same conditions to determine the peak ratio of $A(\text{N}_2 \text{ in the air})/A(\text{O}_2 \text{ in$

the air). The peak area of O₂ from cell leakage was estimated according to the equation of $A(\text{O}_2 \text{ from cell leakage}) = [A(\text{O}_2 \text{ in the air})/A(\text{N}_2 \text{ in the air})] \times A(\text{N}_2 \text{ from cell leakage})$. In this case, the peak area of O₂ from cell leakage could be deducted from the peak area of total O₂, and then the quantity of O₂ generated during the bulk electrolysis experiment was determined with the external standard method. The percentage of O₂ from cell leakage is estimated to be in the range of 0.9% to 16.7% of the total amount of O₂ in the cell during 4 h of electrolysis. The quantity of O₂ from cell leakage increased as the reaction time was extended. According to the O₂ volume evolved and the amount of O₂ calculated from the total consumed charge during the CPE experiment assuming a 4e⁻ catalytic process, the Faradaic efficiencies for electrochemical O₂ evolution are about 96% for **1** and 94% for **2**.

Testing peroxide intermediates formed during CPE experiments in electrolytes.^{S7,S8}

Ampliflu red (AR) was dissolved in DMSO and horseradish peroxidase (HRP) in 0.5 M PBS, both in a concentration of 0.4 mg mL⁻¹. Controlled potential electrolysis (CPE) experiments of **1** or **2** (4 mM) in 0.1 M PBS at pH 7 were carried out at 1.62 V vs. NHE in an electrochemical cell. A fluorine-doped tin oxide (FTO) with a surface area of 2.0 cm² was used as the working electrode. After 2 h of electrolysis, the HRP solution (1.0 mL) and AR solution (1.0 mL) were successively added into the resulting electrolyte (0.3 mL). The color of the solution turned red after the sample was shaken for about 1 minute (Fig. S17).

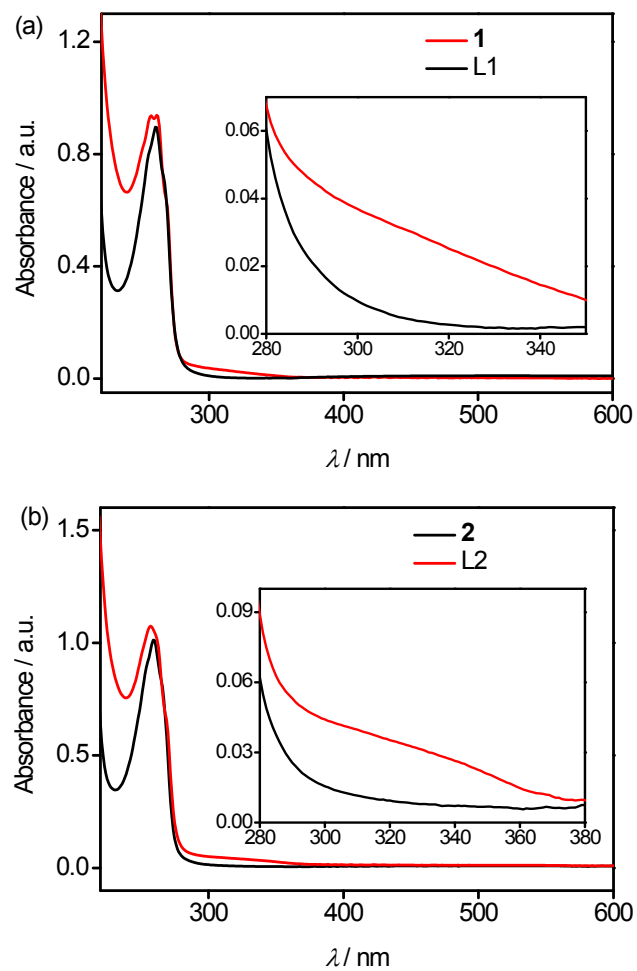


Fig. S1 UV-vis spectra of (a) **1**, **L1** and (b) **2**, **L2** (all in 0.1 mM) in 0.1 M PBS at pH 7. Inset: magnified views of weak absorptions of **1** and **2** in the region of 280–350 and 280–380 nm.

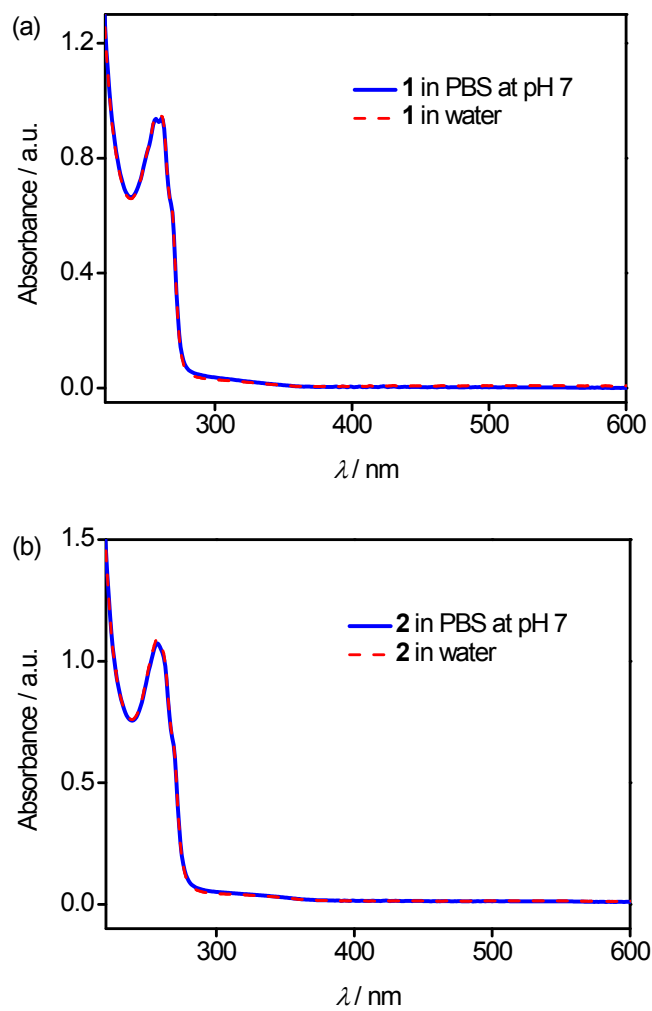


Fig. S2 UV-vis spectra of (a) **1** and (b) **2** (both in 0.1 mM) in 0.1 M PBS at pH 7 and in pure water.

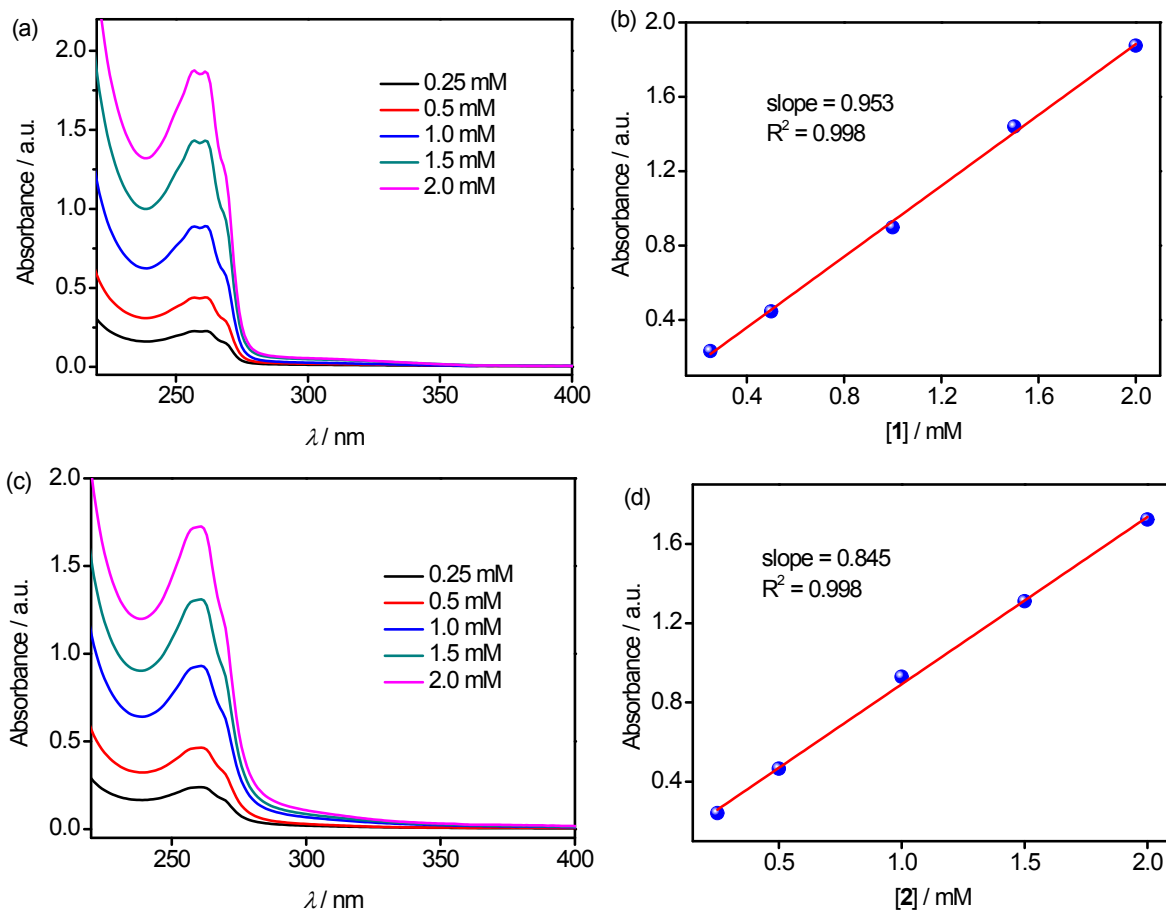


Fig. S3 UV-vis spectra of (a) **1** and (c) **2** in 0.1 M PBS at pH 7.0 in different concentrations of nickel complexes (from 0.25 to 2.0 mM). Plots of the absorbances of (b) **1** at 257 nm and (d) **2** at 260 nm as a function of concentration.

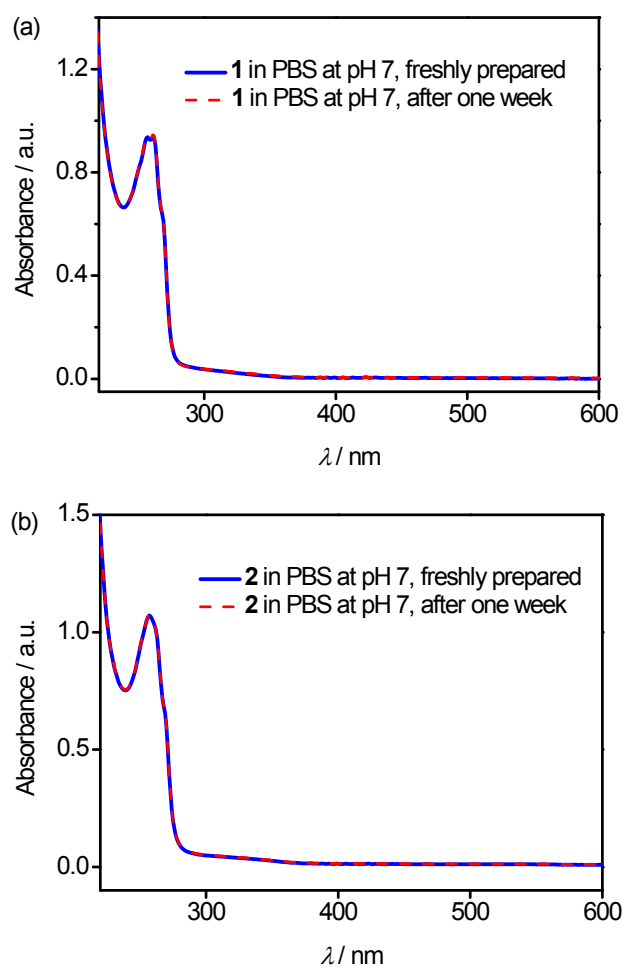


Fig. S4 Comparison of UV-vis spectra of (a) **1** and (b) **2** (both in 0.1 mM) in 0.1 M PBS at pH 7 freshly prepared and after stood for one week under air.

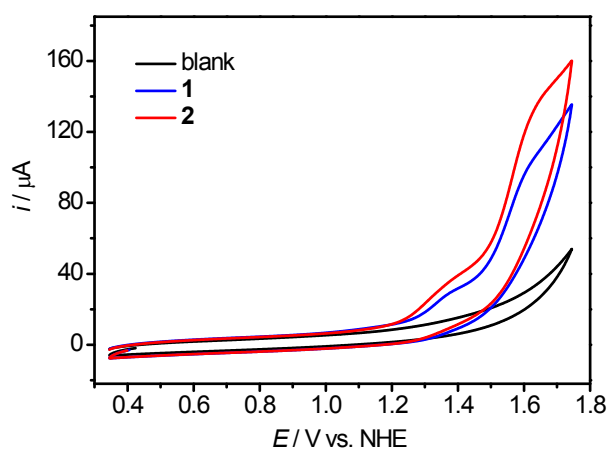


Fig. S5 Cyclic voltammograms of **1** and **2** (both in 0.5 mM) in 0.2 M PBSs at pH 7.0 at a scan rate of 100 mV s^{-1} with a 0.07 cm^2 glassy carbon electrode (To make a fair comparison with the OER activity of $[\text{Ni}(\text{PY5})\text{Cl}]^+$ at pH 7.0, the CVs of **1** and **2** were measured under exactly same conditions as those reported for $[\text{Ni}(\text{PY5})\text{Cl}]^+$, *J. Catal.* 335 (2016) 72–78).

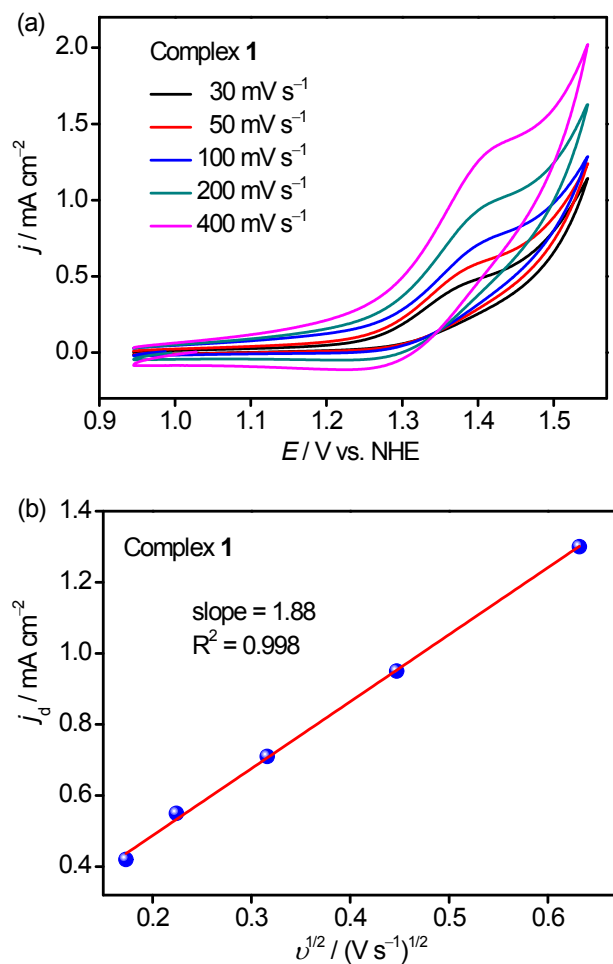


Fig. S6 (a) Cyclic voltammograms of **1** (2.0 mM) in 0.1 M PBSs at pH 7.0 at different scan rates. (b) Plot of the anodic current density maximum of the Ni^{II}/Ni^{III} couple as a function of the square root of scan rate.

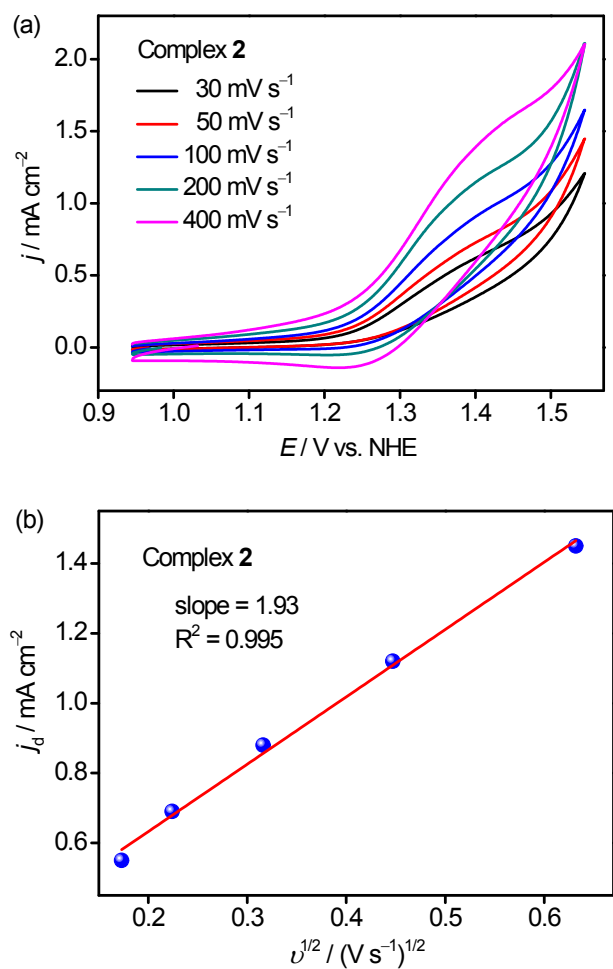


Fig. S7 (a) Cyclic voltammograms of **2** (2.0 mM) in 0.1 M phosphate buffer solutions at pH 7.0 at different scan rates. (b) Plot of the anodic current density maximum of the Ni^{II}/Ni^{III} couple as a function of the square root of scan rate.

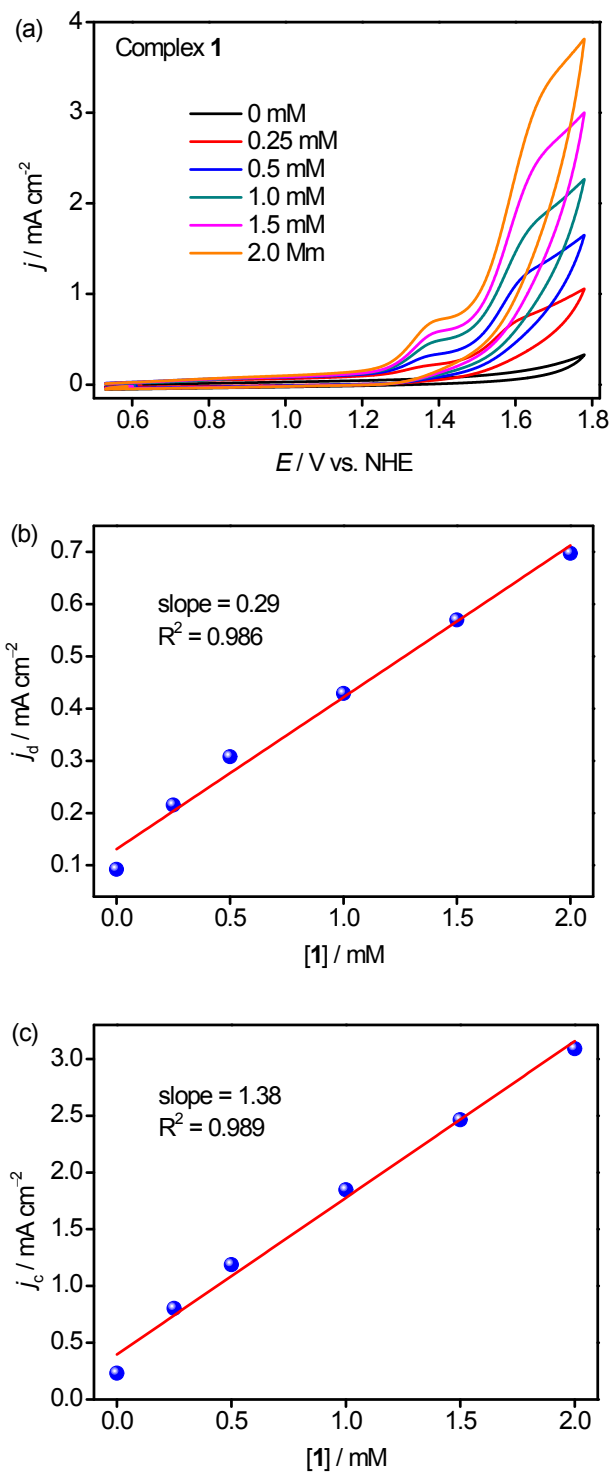


Fig. S8 (a) Cyclic voltammograms of **1** in 0.1 M PBS at pH 7.0 at a scan rate of 100 mV s^{-1} with the concentration of **1** varied from 0 to 2 mM. Plots of the current density maxima of (b) j_d and (c) j_c as a function of catalyst concentration.

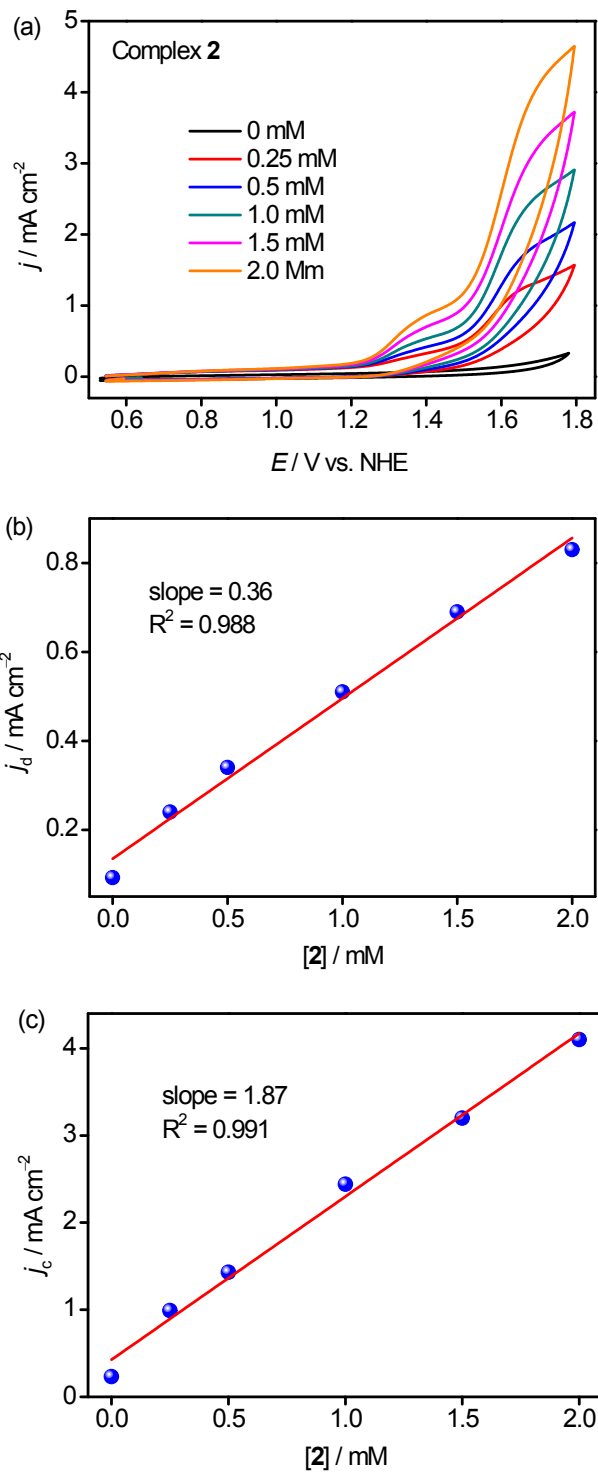


Fig. S9 (a) Cyclic voltammograms of **2** in 0.1 M PBSs at pH 7.0 at a scan rate of 100 mV s^{-1} with the concentration of **2** varied from 0 to 2 mM. Plots of the current density maxima of (b) j_d and (c) j_c as a function of catalyst concentration.

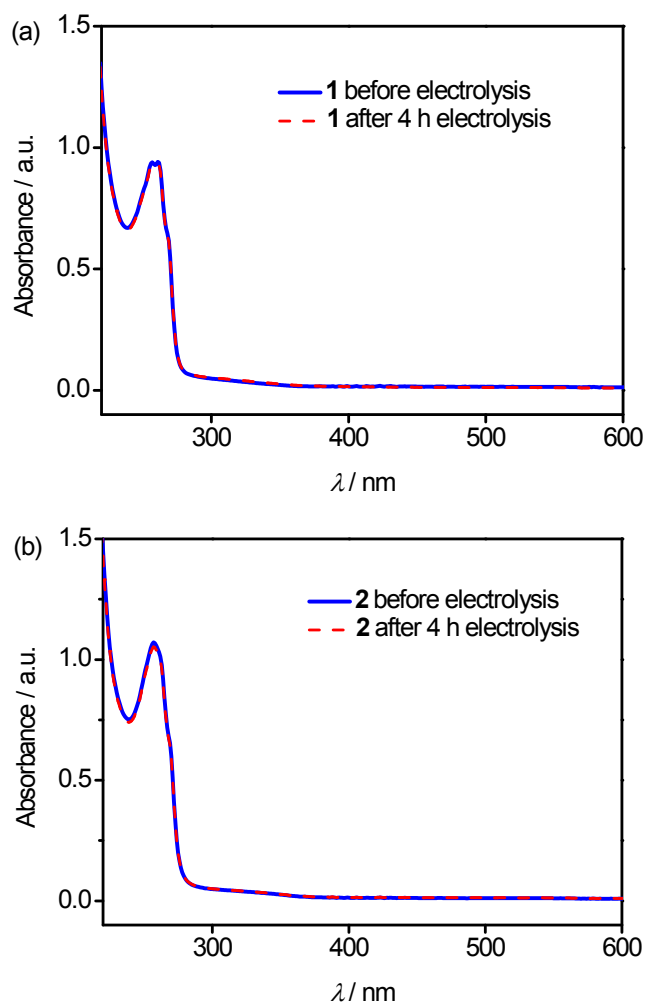


Fig. S10 UV-vis spectra of (a) **1** and (b) **2** (both in 0.1 mM) in 0.1 M PBSs at pH 7.0 before and after electrolysis for 4 h.

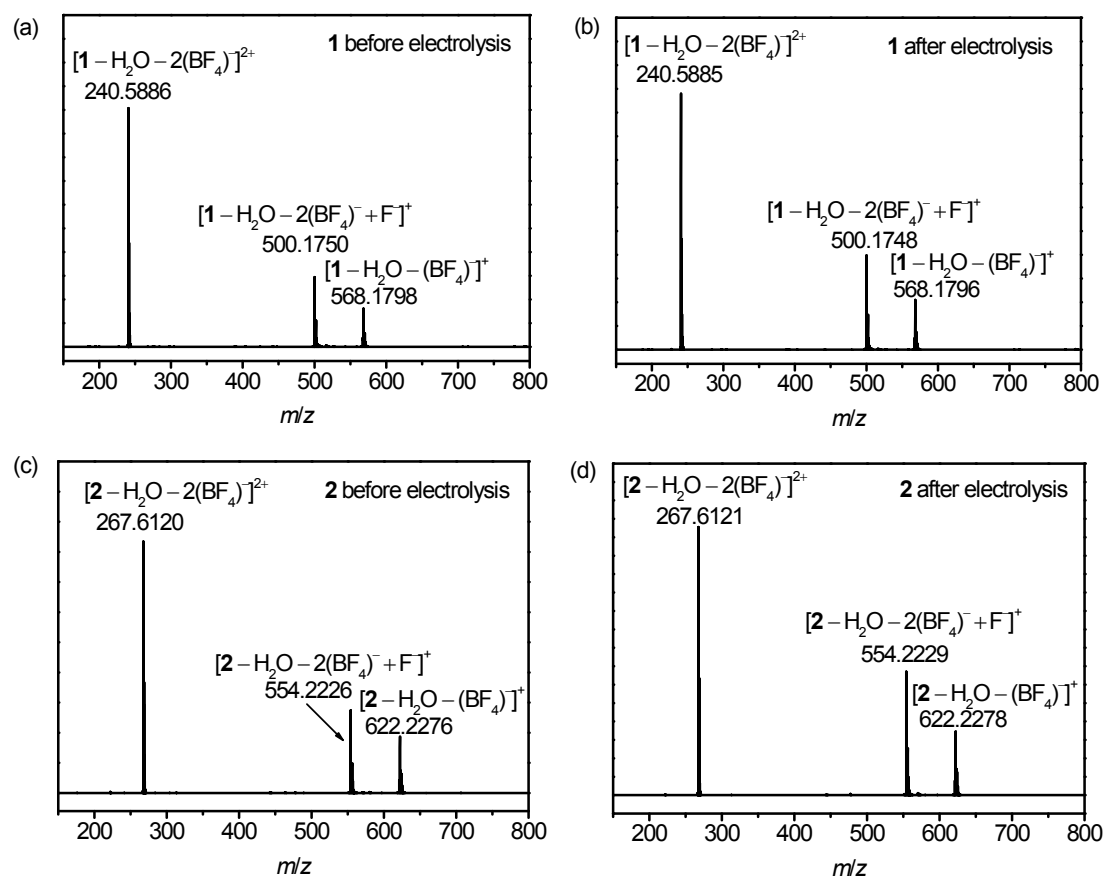


Fig. S11 High-resolution mass spectra of (a,b) **1** and (c,d) **2** in the acetonitrile extract solutions of the dried electrolyte residues (a,c) before and (b,d) after 4 h of electrolysis.

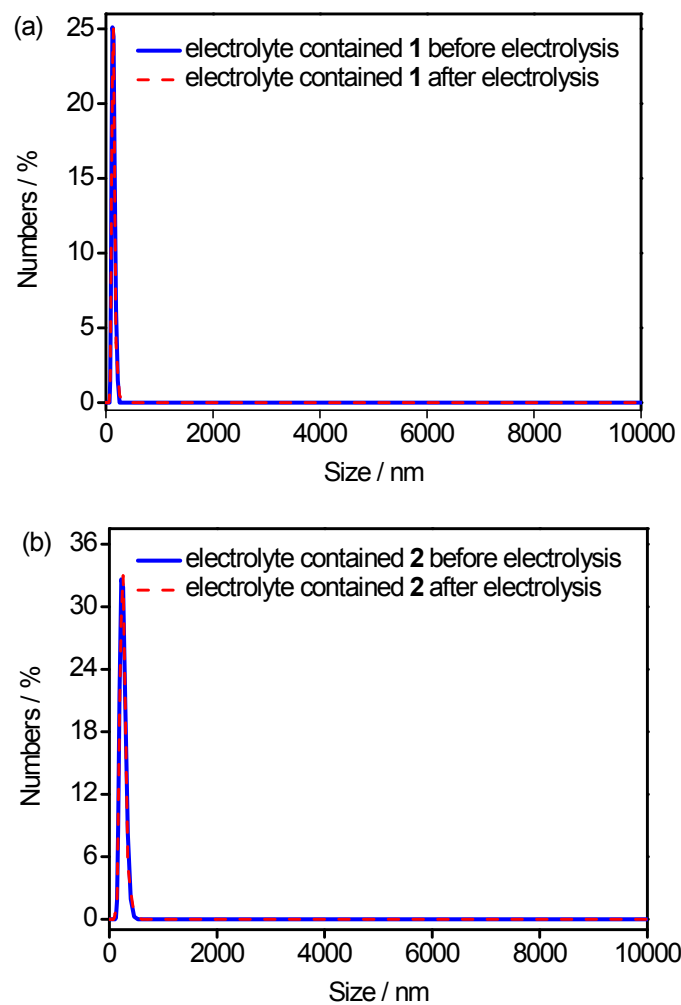


Fig. S12 DLS spectra of the electrolytes containing (a) **1** and (b) **2** before and after 4 h electrolysis.

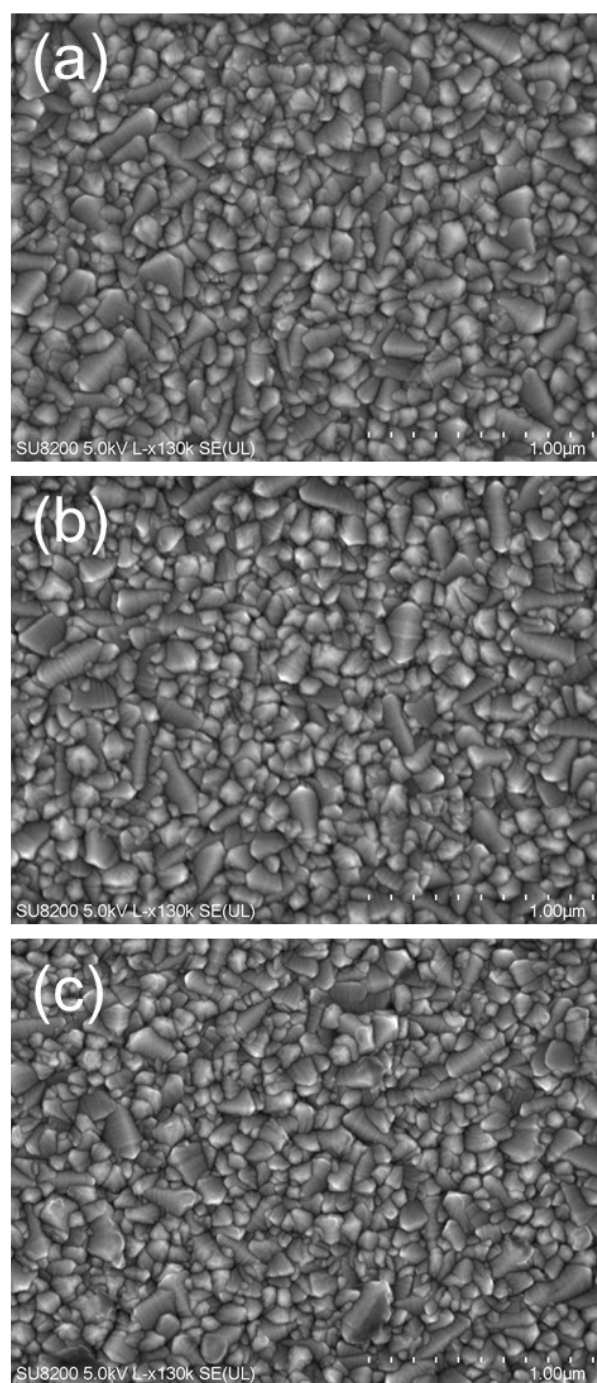


Fig. S13 SEM images of (a) FTOs (a) before and after 4 h of electrolysis with (b) **1** and (c) **2**.

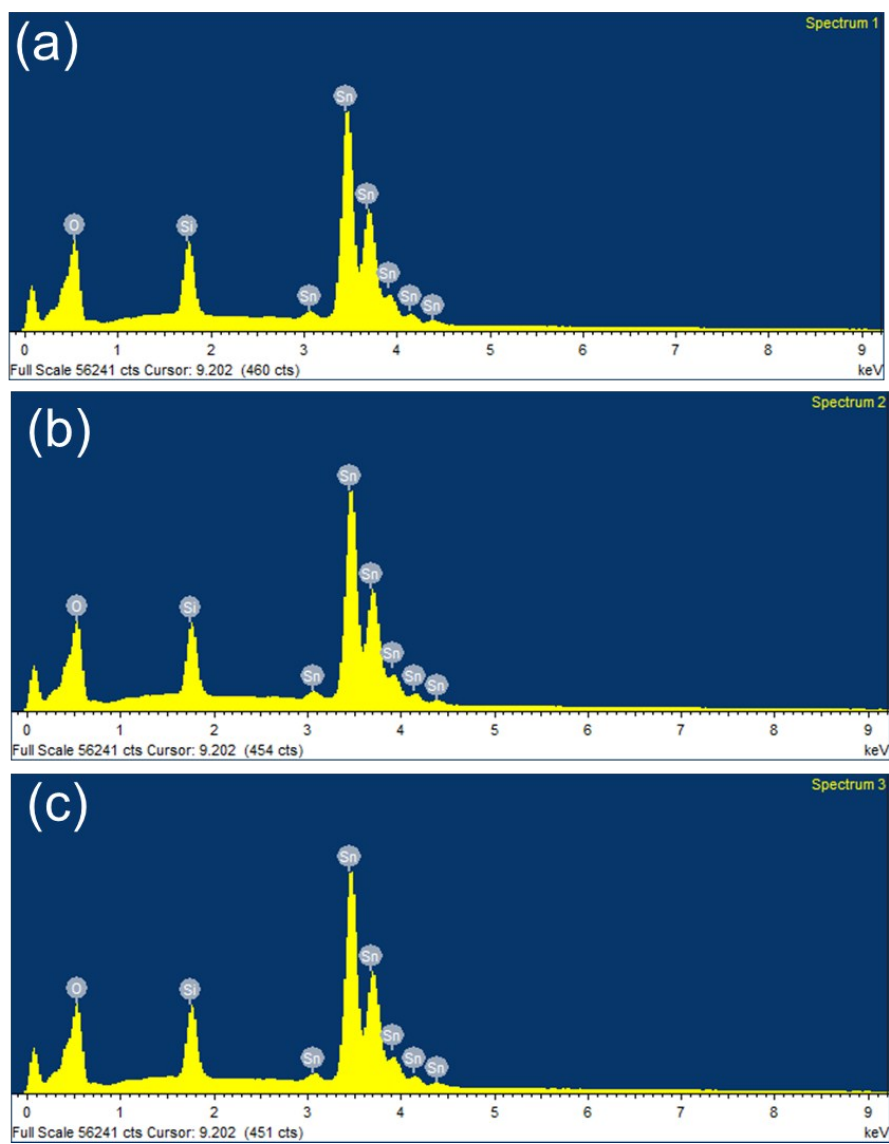


Fig. S14 EDX spectra of FTOs (a) before and after 4 h of electrolysis with (b) **1** and (c) **2**.

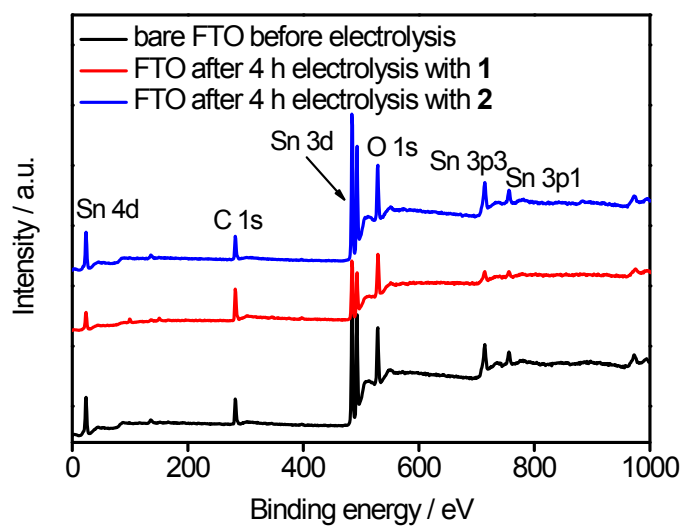


Fig. S15 XPS spectra of FTOs before (black) and after 4 h of electrolysis with **1** (red) and **2** (blue).

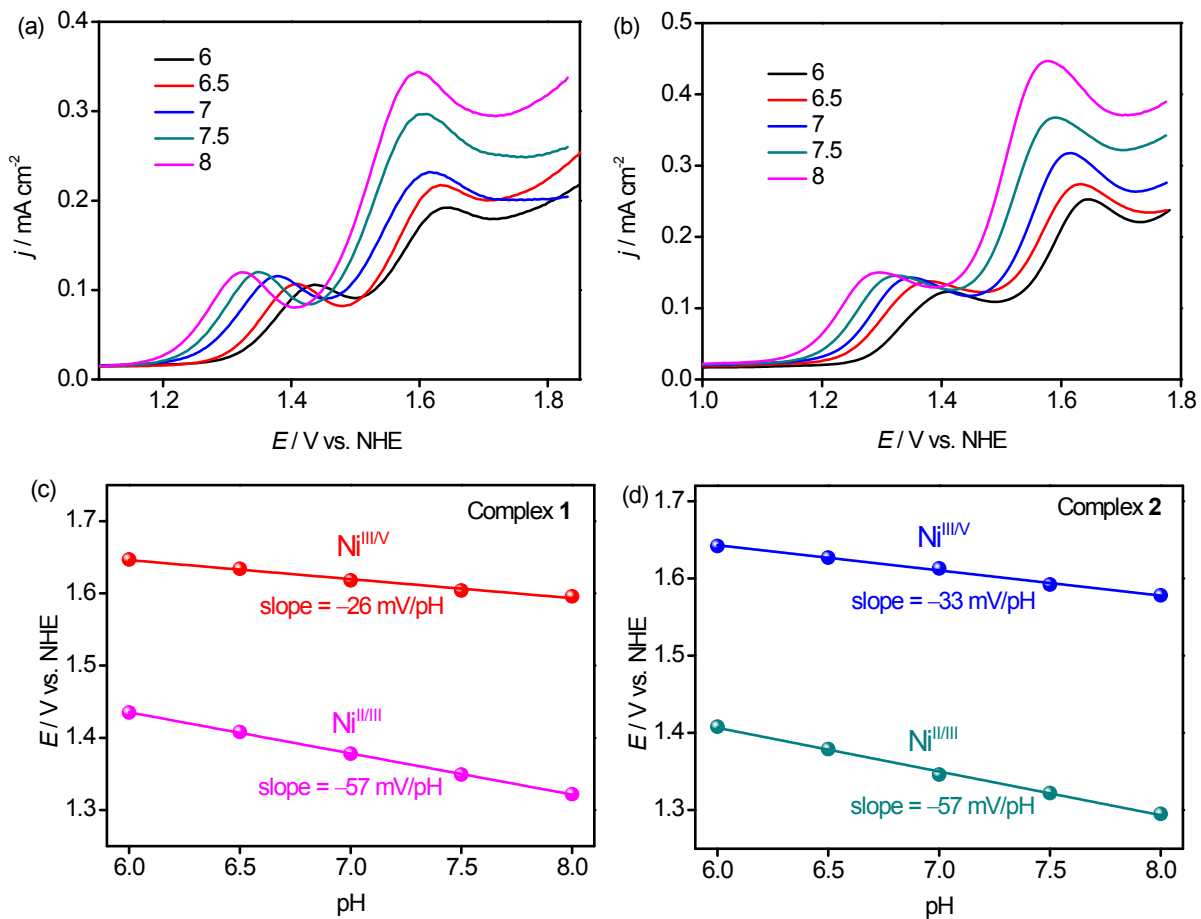


Fig. S16 Differential pulse voltammograms of (a) **1** and (b) **2** (both in 1.0 mM) in 0.1 M PBSs with pH varied from 6 to 8. Pourbaix diagram for (c) **1** and (d) **2**.

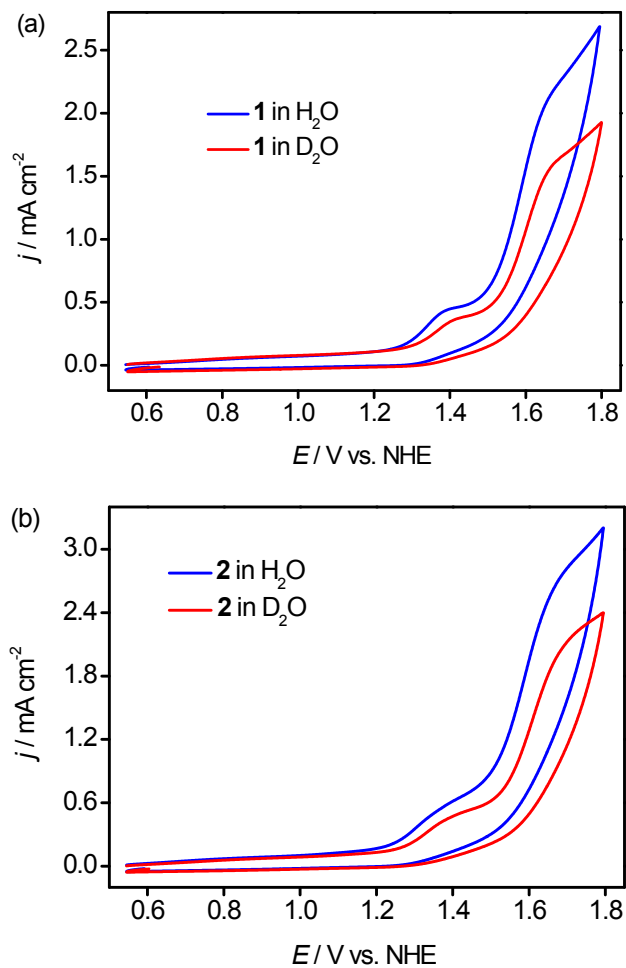


Fig. S17 Cyclic voltammograms of (a) **1** and (b) **2** in H_2O or D_2O phosphate buffer solutions with a glassy carbon plate as the working electrode at a scan rate 100 mV s^{-1} . According to the equation of $k_{\text{cat,H}_2\text{O}}/k_{\text{cat,D}_2\text{O}} = (i_{\text{c,H}_2\text{O}}/i_{\text{c,D}_2\text{O}})^2$, KIE = 1.92 for **1** and 1.87 for **2**.

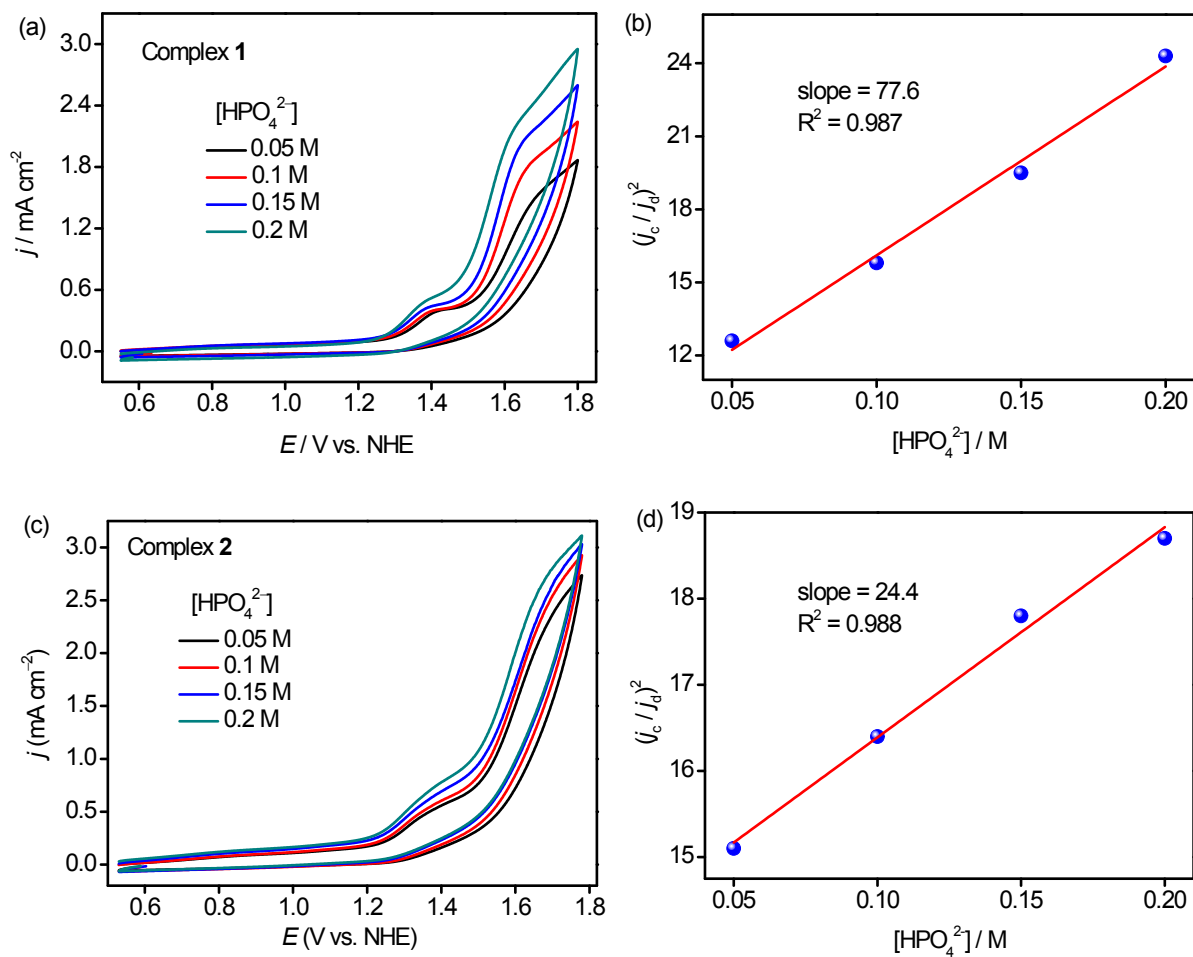


Fig. S18 Cyclic voltammograms of (a) **1** and (c) **2** (both in 1.0 mM) at a scan rate of 100 mV s⁻¹ with the concentration of phosphate buffer solution varied from 0.05 to 0.2 M at pH 7. Plots of $(j_c/j_d)^2$ as a function of $[\text{HPO}_4^{2-}]$ at a constant concentration of (b) **1** and (d) **2**.

Chromogenic Reaction

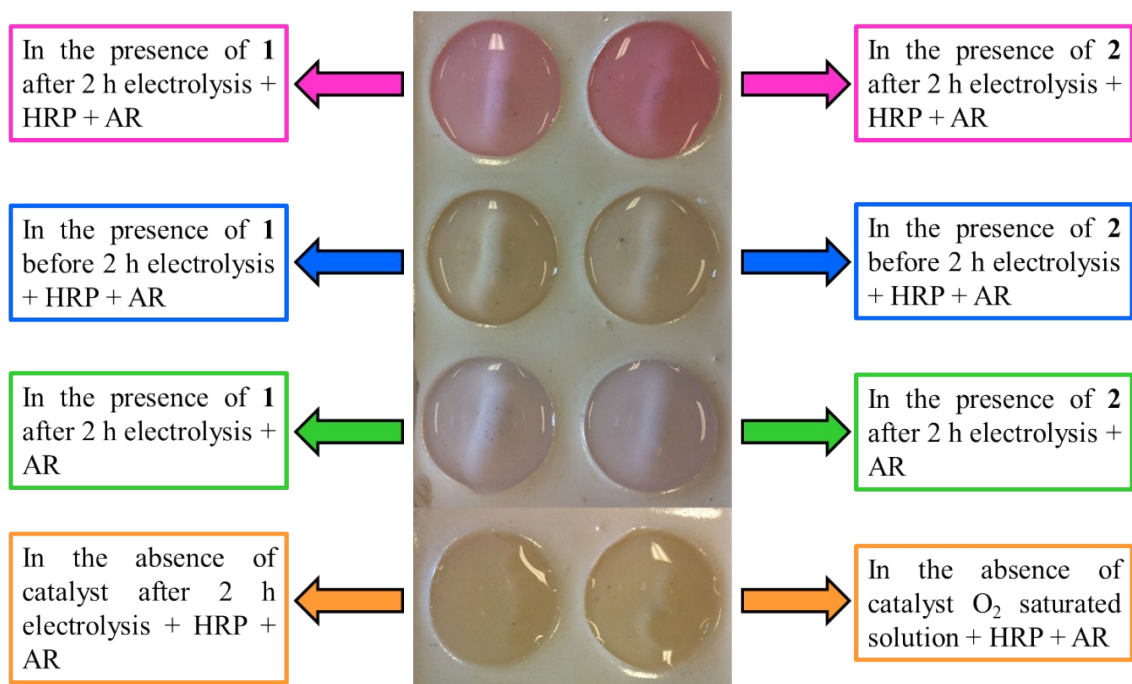


Fig. S19 Chromogenic reactions using horseradish peroxidase (HRP, a special catalyst for hemolysis of the peroxide bond of H₂O₂ to form ·OH radicals) and Ampliflu red (AR, a reliable titrant for ·OH) for testing the hydroperoxide intermediates in the resulting electrolytes after 2 h of electrolysis of **1** and **2** (both in 4 mM) in pH 7 PBSs.

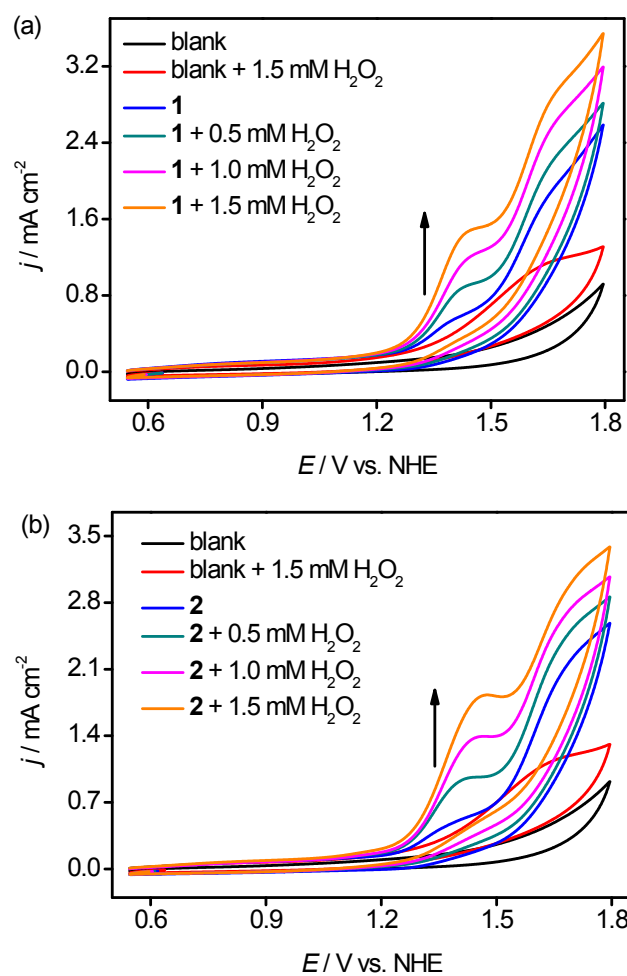


Fig. S20 Cyclic voltammograms of (a) **1** and (b) **2** in 0.1 M PBSs at pH 7 at a scan rate of 100 mV s^{-1} with the increasing concentration of H_2O_2 .

Table S1 Crystallographic data and processing parameters for **1** and **2**

Complex	1 ·H ₂ O	2 ·2H ₂ O
Formula	C ₂₇ H ₃₁ N ₅ OB ₂ F ₈ Ni·H ₂ O	(C ₃₁ H ₃₇ N ₅ OB ₂ F ₈ Ni) ₂ ·2H ₂ O
Formula weight	687.88	1492.00
Crystal system	Orthorhombic	Monoclinic
Space group	Pbcn	P2(1)
<i>Z</i>	8	2
<i>a</i> / Å	10.5139(12)	16.5417(4)
<i>b</i> / Å	14.6832(17)	9.9989(2)
<i>c</i> / Å	40.182(5)	20.3707(5)
<i>α</i> / deg	90.00	90.00
<i>β</i> / deg	90.00	92.5630(10)
<i>γ</i> / deg	90.00	90.00
<i>V</i> / Å ³	6203.3(12)	3365.92(13)
<i>D</i> _{calcd} / g m ⁻³	1.473	1.472
<i>μ</i> / mm ⁻¹	0.708	0.658
Crystal size / mm	0.24 × 0.17 × 0.12	0.31 × 0.28 × 0.26
<i>θ</i> Range / deg	2.03 / 27.51	2.35 / 25.00
Reflns collected / Indep.	39721/7120	31452 / 9906
Parameters refined	406	907
<i>F</i> (000)	2816	1544
GOF on <i>F</i> ²	1.023	1.025
Final <i>R</i> ₁ (<i>I</i> > 2(<i>I</i>))	0.0677	0.0624
Final <i>wR</i> ₂ (<i>I</i> > 2(<i>I</i>))	0.1906	0.1561
max. peak/hole / e Å ⁻³	0.813/ -0.522	1.708 / -0.868

$$R_1 = \frac{\sum||F_o| - |F_c||}{\sum|F_o|}, wR_2 = \left[\frac{\sum(|F_o|^2 - |F_c|^2)^2}{\sum(F_o^2)}\right]^{1/2}$$

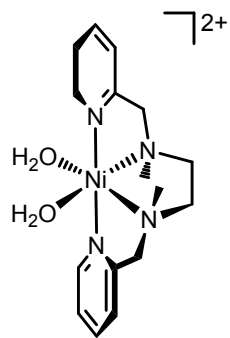
Table S2 Selected bond lengths (Å) and angles (deg) for **1** and **2**

Complex 1 ^{S3}		Complex 2	
Bond lengths (Å)		Bond lengths (Å)	
Ni–N1	2.100(3)	Ni–N1	2.086(5)
Ni–N2	2.102(3)	Ni–N2	2.093(5)
Ni–N3	2.079(3)	Ni–N3	2.145(4)
Ni–N4	2.175(3)	Ni–N4	2.164(4)
Ni–N5	2.077(3)	Ni–N5	2.104(4)
Ni–O1	2.073(3)	Ni–O1	2.073(5)
Bond angles (deg)		Bond angles (deg)	
N1–Ni–N2	79.91(13)	N1–Ni–N2	79.28(19)
N1–Ni–N3	93.45(12)	N1–Ni–N3	89.17(18)
N1–Ni–N4	163.10(12)	N1–Ni–N4	156.7(2)
N1–Ni–N5	89.38(12)	N1–Ni–N5	94.52(17)
N2–Ni–N3	95.61(13)	N2–Ni–N3	102.92(19)
N2–Ni–N4	84.83(11)	N2–Ni–N4	84.70(18)
N2–Ni–N5	82.12(13)	N2–Ni–N5	80.71(18)
N3–Ni–N4	80.80(12)	N3–Ni–N4	77.94(16)
N3–Ni–N5	176.02(12)	N3–Ni–N5	175.27(19)
N4–Ni–N5	95.71(12)	N4–Ni–N5	99.54(16)
N1–Ni–O1	99.07(13)	N1–Ni–O1	101.1(2)
N2–Ni–O1	175.39(12)	N2–Ni–O1	171.19(17)
N3–Ni–O1	88.93(12)	N3–Ni–O1	85.89(19)
N4–Ni–O1	96.71(11)	N4–Ni–O1	97.33(19)
N5–Ni–O1	93.38(12)	N5–Ni–O1	90.50(18)

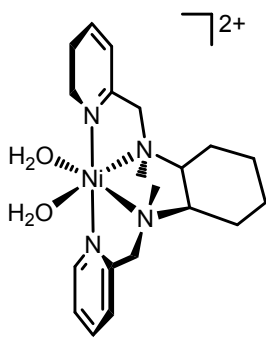
Table S3 Performance of nickel complexes reported as water oxidation catalysts

Catalyst ^a	η at 1.0 mA cm ⁻²	j (mA cm ⁻²) at η = 780 mV	CPE	TON, k_{cat} or k_{obs}	Conditions	Ref.
[Ni(<i>meso</i> -L)] ²⁺	~ 534 mV	~ 1.12	0.9 mA cm ⁻² at η = 734 mV	15 (6 h at η = 734 mV)	0.1 M PBS, pH 7, 1 mM catalyst	S9
[Ni(L1)] ²⁺	~ 730 mV ^b	~ 1.13	0.28 mA cm ⁻² at η = 681 mV	–	0.1 M carbonate, pH 7, 1 mM catalyst	S10
[Ni(Me ₈ L)] ²⁺	~ 660 mV	~ 1.35	1.05 mA cm ⁻² at η = 750 mV	15.2 (5 h at η = 734 mV)	0.1 M PBS, pH 7, 1 mM catalyst	S11
[Ni(<i>mep</i>)(H ₂ O) ₂] ₂₊	~ 670 mV	~ 1.62	0.2 mA cm ⁻² at η = 383 mV	3.4 (33 h at η = 755 mV)	0.3 M acetate, pH 6.5, 1 mM catalyst	S12
[Ni(<i>mcp</i>)(H ₂ O) ₂] ₂₊	~ 730 mV	~ 1.24	0.42 mA cm ⁻² at η = 680 mV	0.19 s ⁻¹	0.1 M PBS, pH 7, 1 mM catalyst	S13
[Ni(L)(H ₂ O) ₂] ⁺	~ 900 mV	~ 0.53	from 0.7 to 0.1 mA cm ⁻² at η = 884 mV	0.15 s ⁻¹	0.1 M PBS, pH 7, 0.5 mM catalyst	S14
[Ni(Por-Hpy ₄)] ⁴⁺	0.56 mA cm ⁻² at ~ 540 mV	–	75 μ A cm ⁻² at η = 500 mV	~ 0.67 s ⁻¹	0.1 M PBS, pH 7, 0.9 mM catalyst	S15
[Ni(PY5)Cl] ⁺	~ 860 mV	~ 0.66	1.7 mA cm ⁻² at η = 910 mV	145 s ⁻¹	0.2 M PBS, pH 10.8, 0.5 mM catalyst	S16
[Ni(L2)] ²⁻	0.6 mA cm ⁻² at ~ 921 mV	~ 0.45	0.23 mA cm ⁻² at η = 480 mV	0.4 s ⁻¹	0.2 M PBS, pH 11, 1.5 mM catalyst	S17
1	730 mV	1.68	0.50 mA cm ⁻² at η = 800 mV	3.06 s ⁻¹	0.1 M PBS, pH 7, 1 mM catalyst	This work
2	702 mV	1.96	0.67 mA cm ⁻² at η = 800 mV	4.62 s ⁻¹		

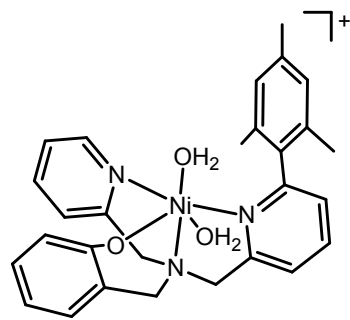
^a The structures of the nickel catalysts are listed below.



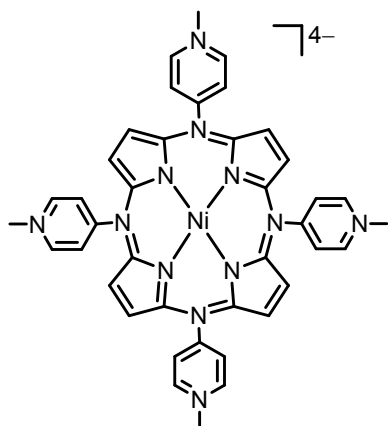
$[Ni(mep)(H_2O)_2]^{2+}$



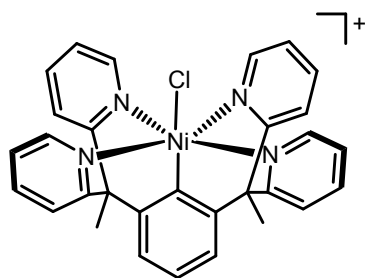
$[Ni(mcp)(H_2O)_2]^{2+}$



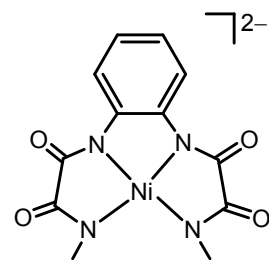
$[Ni(L)(H_2O)_2]^+$



$[Ni(TPPE)]^{4-}$



$[Ni(PY5)Cl]^+$



$[Ni(L2)]^{2-}$

References

- [S1] L. Duelund, R. Hazell, C. J. McKenzie, L. P. Nielsen and H. Toftlund, *J. Chem. Soc., Dalton Trans.*, 2001, 152.
- [S2] A. Mohamadi and L. W. Miller, *Tetrahedron Lett.*, 2017, **58**, 1441.
- [S3] P. Zhang, M. Wang, Y. Yang, D. Zheng, K. Han and L. Sun, *Chem. Commun.*, 2014, **50**, 14153.
- [S4] G. M. Sheldrick, *SHELXTL97 Program for the Refinement of Crystal Structure*, University of Göttingen, Germany, **1997**.
- [S5] *Software packages SMART and SAINT*, Siemens Energy & Automation Inc., Madison, Wisconsin, **1996**.
- [S6] G. M. Sheldrick, *SADABS Absorption Correction Program*, University of Göttingen, Germany, **1996**.
- [S7] V. Mishin, J. P. Gray, D. E. Heck, D. L. Laskin and J. D. Laskin, *Free Radical Biology & Medicine*, 2010, **48**, 1485.
- [S8] U. S. Akhtar, E. L. Tae, Y. S. Chun, I. C. Hwang and K. B. Yoon, *ACS Catal.*, 2016, **6**, 8361.
- [S9] M. Zhang, M.-T. Zhang, C. Hou, Z.-F. Ke and T.-B. Lu, *Angew. Chem., Int. Ed.*, 2014, **53**, 13042.
- [S10] B. Ariela, W. Yaniv, S. Dror, K. Haya, A. Yael, M. Ericb and M. Dan, *Dalton Trans.*, 2017, **46**, 10774.
- [S11] J.-W. Wang, C. Hou, H.-H. Huang, W.-J. Liu, Z.-F. Ke and T.-B. Lu, *Catal. Sci. Technol.*, 2017, **7**, 5585.
- [S12] G.-Y. Luo, H.-H. Huang, J.-W. Wang and T.-B. Lu, *ChemSusChem*, 2016, **9**, 485.
- [S13] J.-W. Wang, X.-Q. Zhang, H.-H. Huang and T.-B. Lu, *ChemCatChem*, 2016, **8**, 3287.
- [S14] D. Wang and C. O. Bruner, *Inorg. Chem.*, 2017, **56**, 13638.

[S15] Y. Han, Y. Wu, W. Lai and R. Cao, *Inorg. Chem.*, 2015, **54**, 5604.

[S16] L. Wang, L. Duan, R. B. Ambre, Q. Daniel, H. Chen, J. Sun, B. Das, A. Thapper, J. Uhlig, P. Dinér and L. Sun, *J. Catal.*, 2016, **335**, 72.

[S17] J. Lin, P. Kang, X. Liang, B. Ma and Y. Ding, *Electrochim. Acta*, 2017, **7**, 353.